Publications

Available Online

J. Sci. Res. **13** (3), 923-933 (2021)

JOURNAL OF SCIENTIFIC RESEARCH

www.banglajol.info/index.php/JSR

DFT and TD-DFT Study of Only First Diaminomalenonitrile Based Molecular Receptor for Fluoride Anion: Correlation of Calculated and Experimental Results

M. A. Kaloo[1,2*], H. Basheer[1], M. A. Rather[2], S. A. Majid[1], B. A. Bhat[1*]

[1]Department of Chemistry, Govt. Degree College Shopian, 192303-Kashmir, India

[2]Department of Chemistry, Govt Degree College Doda, 182202-Jammu, India

Received 7 November 2020, accepted in final revised form 30 June 2021

Abstract

In this work, the sensing mechanism of a novel anion receptor, 2-amino-((E)-(4-cyanobenzalidine) amino) maleonitrile reported by Sankar *et al*. (Analyst 138:4760-4763, 2013) was investigated theoretically with the help of density functional theory (DFT) and time-dependent density functional theory (TD-DFT). From the frontier molecular orbital analysis, it is reasonable to support the proposed charge transfer (ICT) enhancement in the receptor molecule in the presence of F^-. A significant reduction in the energy gap (ΔE) from 4.014 eV to 2.342 eV between highest occupied and lowest unoccupied energy levels was revealed, leading to the strong redshift of its absorption characteristics. Moreover, ^{1}H NMR was also calculated to further understand the mechanistic insights by using the gauge independent atomic orbital (GIAO) method with B3LYP methods and the 6-311^{++}G (*d*,*p*) basis set. The spectra were simulated, and the chemical shifts linked to TMS were compared with experimental. Besides, Intrinsic Reaction Coordinates (IRC) were also calculated to understand the sensing mechanism.

Keywords: Receptor; Diaminomalenonitrile; DFT; Absorption; Proton transfer; Fluoride; Simulation.

© 2021 JSR Publications. ISSN: 2070-0237 (Print); 2070-0245 (Online). All rights reserved.
doi: http://dx.doi.org/10.3329/jsr.v13i3.50183 J. Sci. Res. **13** (3), 923-933 (2021)

1. Introduction

Anions are ubiquitous and play important roles in a myriad of biological, chemical, environmental, and pathological processes [1-3]. Sensing of such chemical entities with the aid of easy to synthesize abiotic molecules "receptors" approaches has been established to be of utmost importance. This is attributed to the fact that such strategies hold the potential to overcome the requirement of bulky and sophisticated instrumentation, tedious and sample preconcentration, delayed signal readout, and high detection limits [4-6]. The most common and easiest molecular receptor design for sensing anions like fluoride (F^-), cyanide (CN^-), and acetate (CH_3COO^-) involve polarization of N–H bond in a range of functionalities like amides, ureas, thioureas,

*Corresponding author: makandchem@gmail.com (MAK); barbilal20@gmail.com (BAB)

ammonium, imidazole and in imidazolium compounds [7-12]. Such systems are well established to detect the anions through hydrogen bonding and/or proton transfer (PT) mechanism in polar aprotic solvents [13,14]. Among these anions, the recognition of F^- has particular interest because of its crucial role in osteoporosis, fluorination of drinking water, chemical and nuclear warfare agents, etc. [15-17]. Besides, excess F^- causes immune system disruption, fluorosis of bone, kidney damage, urolithiasis, and even cancer [18,19].

For the recognition of fluoride, an unprecedented molecular anion receptor with polarized N-H bond in the free NH_2 functionality, 2-Amino-((E)-(4-cyanobenzalidine) amino) maleonitrile (named **1** herein) was reported by Sankar *et al.* [20]. The molecular system with a highly extensively conjugated framework belongs to a class of organic π-conjugated compounds with electronic donor (D) and acceptor (A) parts connected by single and double bonds. Such D-π-A molecules are push-pull systems and exhibit interesting electronic properties due to intramolecular charge transfer (ICT) processes. These ICT chromophores being highly robust with exceptional light, heat, and weather stability, have been intensively studied as tunable materials for non-linear optics (NLO), optical data storage devices, organic light-emitting diodes (OLED), organic-inorganic hybrid materials, and functional polymers. The novel receptor (Fig. 1) could recognize F^- via both absorptions as well emission readout. However, emission changes were not strong enough to detect F^-through naked-eyes, contrary to the colorimetric output signal, which was prompt and suitable to detect anion even at low concentrations (20-50 μM). The mechanism responsible for naked-eye recognition of F^- was reported to be proton transfer from **1** to F^-. In effect, as far as a new receptor design in anion recognition chemistry, mechanistic investigations are necessary for prospective and futuristic applications. In addition to this, indirect information about photophysical and photochemical characteristics of the molecule before and after ion recognition can be afforded based upon theoretical calculations. Therefore, it is necessary to study the reported receptor through a quantum computational approach (DFT/TD-DFT) [21-24]. Importantly, to the best of our knowledge, no such report exists wherein anion receptors designed from DAMN molecular backbone possessing free $–NH_2$ moiety have been investigated theoretically besides experimental. In this work, we have tried to fill this gap and further understand the experimental insights of **1** and its naked-eye sensing characteristics towards F^- under the polar aprotic solvent system (THF herein).

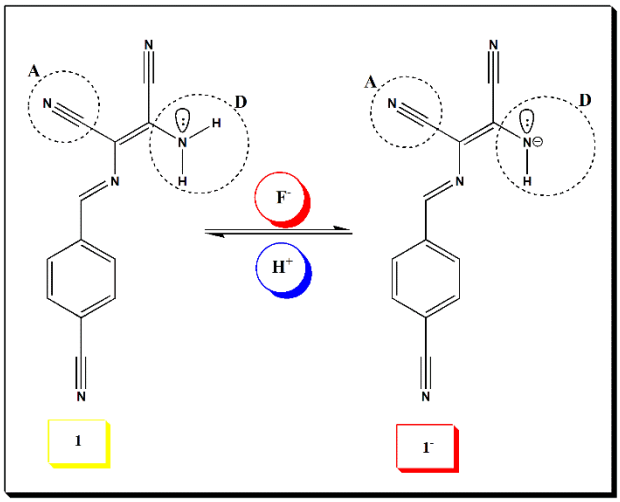

Fig. 1. Proposed mechanism of F^-interaction with the molecular receptor (**1**) leading to the formation of deprotonated receptor $\mathbf{1}^-$, and its reversal in the presence of acid (H^+).

2. Computational Details

All calculations were performed using Gaussian 09 program [25]. The hybrid density functional theory (DFT) and Time-Dependent DFT (TD-DFT) calculations were run for the excited state and electronic spectra. B3LYP/6-31G+ (d,p) was used to obtain the geometry optimization and IRC parameters of the **1** as it is moderate and suitable for such organic molecular structures [26]. The geometry optimization and IRC parameters of the deprotonated form of receptor $\mathbf{1}^-$ were also carried out with the same method. To investigate the solvent effect of THF, PCM (polarized continuum model) calculation was performed throughout the steps [27,28]. In addition, ^{1}H NMR calculations were performed at MPW1PW91/6-311+G (*d,p*) level along with the gauge-independent atomic orbital (GIAO) method.

3. Results and Discussion

3.1. *Optimized structures*

The optimized structures of **1** and deprotonated form of the receptor, $\mathbf{1}^-$ are shown in Fig. 2. The ground state (S_0) ionization energies (I. Es) of **1** and $\mathbf{1}^-$ are found to be -735.17 and -830.26 A.U., respectively. The bond distance between N_{19}–H_{20} and N_{19}-H_{21} in **1** ground state optimized structure and exciting structure seem to be equidistant, i.e., 0.99 Å. In the ground state of $\mathbf{1}^-$, an increase in the bond distance between hydrogen and nitrogen was found, i.e., 1.033 Å, which attributes to the increase in the electronic density of nitrogen. The bond C-N (NH_2) bond distance is equal to (1.47 Å) in receptor **1.** However, in the case of $\mathbf{1}^-$, it decreases to 1.36 Å, which attributes to higher bond order between C-N. The

important structural parameters (bond length and bond angles) of **1** and **1**$^-$ are further summarized in Table 1.

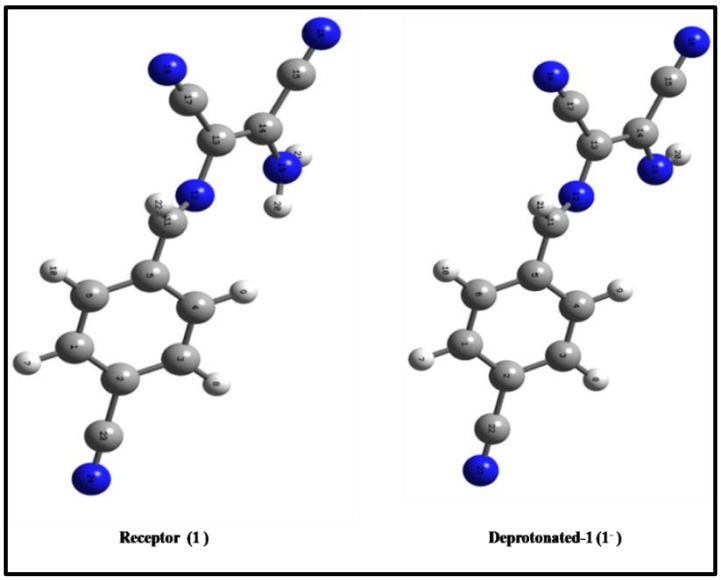

Fig 2. Optimized structures of receptors **1** and **1**$^-$.

Table 1. The structural parameters (bond length, L and bond angle, Θ) in the optimized geometry of **1** and **1**$^-$.

C-N (L)	C=N (L)	C=C (L)	Ph-C≡N (L)	N-H (L)	C-N-C (Θ)	N-C-H (Θ)
11.47	1.29	1.316	1.16	0.99	125.7	120.9
11.36	1.29	1.416	1.16	1.03	120.1	120.40

3.2. *UV–Vis spectra and molecular orbital analysis*

Experimental studies with UV-Vis spectra of **1** and **1**$^-$ revealed a redshift of its characteristic absorption band (λ_{max}**)** from 376 to 465 nm [29]. Such a spectral shift (**Δλ)** of 89 nm was proposed to occur as a result of proton transfer signaling (PTS) from amine hydrogen (NH–H) of **1** to the fluoride. Due to the strong basic nature of F^- in polar aprotic solvents, the interaction of F^- results in the formation of negatively charged molecular species (named herein **1**$^-$ in Fig. 1). The concentration of negative charge density on the amine nitrogen results in the enhancement of the electronic push-pull effect between the donor (D) amine moiety and acceptor (A) nitrile (CN) functionality. The facilitation of such *D-π-A* interaction is responsible for visual and prompt colorimetric sensing of F^-.

In order to investigate these photophysical characteristics of receptors in the presence and absence of fluoride anion (**1** to **1**$^-$**)**, a molecular excitation study of both these molecules was carried out (Figs. 3 and 4, respectively). Simulated spectra of receptor **1**

show an intense absorption peak at 336 nm as a dominant π-π* type transition with the oscillator strength (*f*) of 0.4162, which is from the highest occupied molecular orbital (HOMO) to the lowest unoccupied molecular orbital (LUMO). The calculated wavelength of absorption maximum corresponds to the energy gap (ΔE) of 4.014 eV. The *pi*-electron density in the HOMO delocalized both through phenyl moiety and an amine group. In the local transition, these delocalized electrons (HOMO) were transited only to phenyl moiety (LUMO). However, in $\mathbf{1}^-$, an intense absorption peak at 493 nm was obtained, resulting from dominant π-π* type transition from the highest occupied molecular orbital (HOMO) to the lowest unoccupied molecular orbital (LUMO) with 2.342 eV energy gap. The corresponding oscillator strength was calculated to be $f = 0.0184$. Thus, the decrease in the energy gap between HOMO and LUMO of receptor in the presence of F^- realizes a strong spectral shift (redshift), and hence offering naked-eye optical detection of anions.

In addition to the HOMO to LUMO transition in both the neutral and deprotonated receptor molecule, other transitions with minor contributions towards photophysical behavior were also calculated (Fig. 3a**)**. The second dominant transition in **1** occurs from HOMO-1 to LUMO with ΔE = -3.837 eV. Other fewer energy transitions include HOMO-2, LUMO, and HOMO to LUMO + 1 with ΔE of 3.865 eV and 3.216 eV, respectively. Similarly, HOMO-1 to LUMO, HOMO-2 to LUMO, HOMO to LUMO + 1 transition in the deprotonated form of the **1** have been shown in Fig. 3b.

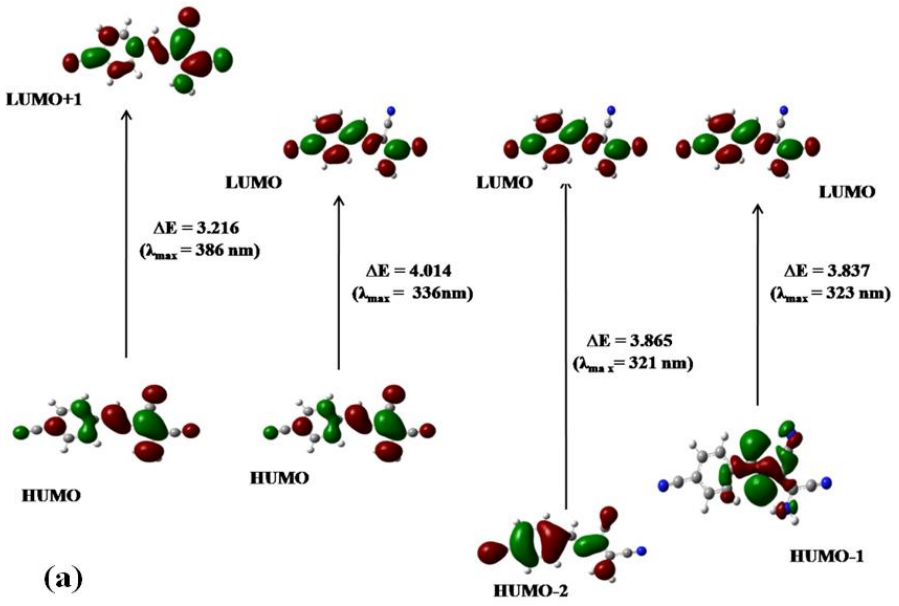

Fig. 3(a) Frontier molecular orbitals of the receptor, **1** before in the absence of F^-. The energy gap (ΔE) between corresponding transitions and their maximum absorption wavelengths are mentioned herein.

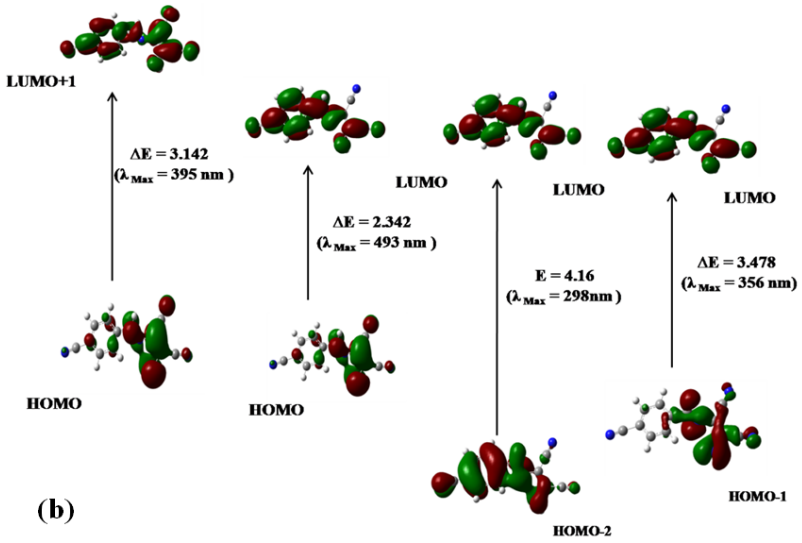

Fig. 3. (b) frontier molecular orbitals of receptor in the presence of F^- (**1**$^-$). The energy gap (ΔE) between corresponding transitions and their maximum absorption wavelengths are mentioned herein.

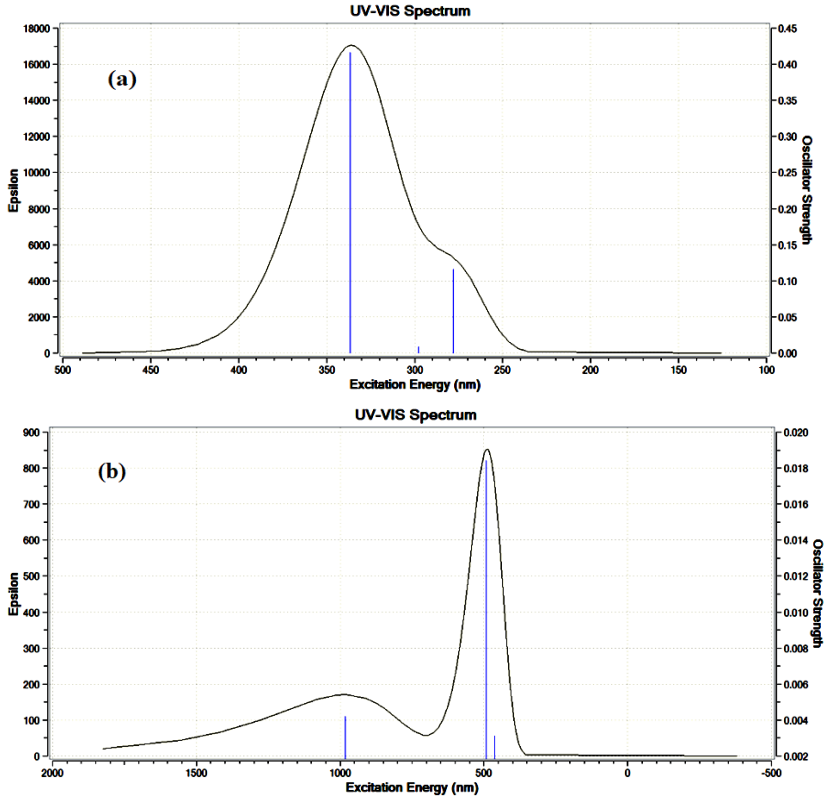

Fig. 4. (a) Simulated absorption spectra (UV-Vis) of receptor **1** in THF and (b) simulated absorption spectra (UV-Vis) of the deprotonated form of the receptor, **1**$^-$ in THF.

3.3. *^{1}H NMR spectra studies*

To reveal the deprotonation mechanism in the fluoride ion sensing, ^{1}H NMR calculations were performed at the MPW1PW91/6-311+G (d,p) level and with the gauge-independent atomic orbital (GIAO) method for **1** and **1**$^-$. The calculated results were further compared with experimental data. For **1**, the ^{1}H NMR signals at 8.27 ppm are assigned to the equivalent protons of the NH_2. Whereas in the case of **1**$^-$, the N-H signal shifted to 22.23 ppm, whereas the phenyl-C-H protons also shifted to up-field. The aromatic proton signals also shifted to upfield, implicating PT and induced charge transfer (ICT). The calculated NMR spectra (Fig. 5) of **1** and **1**$^-$ agree quite good with experimental observations [30]. Thus, it is evidenced that in the presence of fluoride ion, the hydrogen atom is transferred from **1** to the fluoride anion to form a deprotonated structure, **1**$^-$. This transfer of proton results, in turn, results in the enhancement of ICT across the receptor. The important data is tabulated below in Table 2.

Table 2. ^{1}H NMR data of **1** and **1**$^-$.

Proton	Receptor (**1**) (Shift)	**1**$^-$ (Shift)
H_7	8.06	8.02
H_8	8.01	8.00
H_9	8.00	8.23
H_{10}	7.89	7.88
H_{20}	4.45 (NH_2)	-
H_{21}	4.45 (NH_2)	-
H_{22}	8.67 (C-H)	8.75

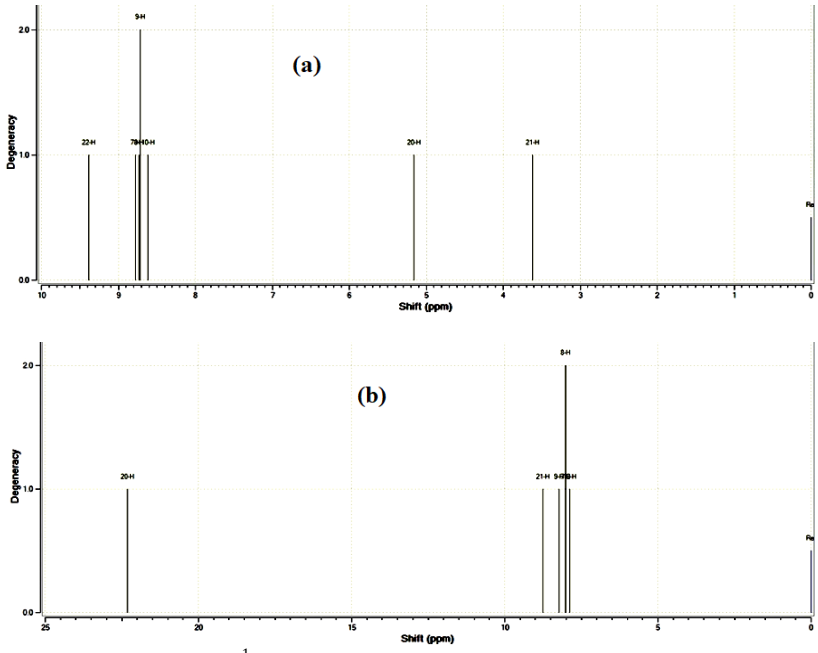

Fig. 5. (a) Theoretically calculated ^{1}H NMR of Receptor **1** and (b) deprotonated form of the receptor, **1**$^-$.

3.4. *Transition state and IRC calculations*

In order to capture the dynamic feature of the proton transfer reaction, Gibb's free energy in the solution was calculated. The ground state Gibb's free energy of the **1** and $\mathbf{1}^-$ were found to be -1.171 kcal/mol and -1.323 kcal/mol, respectively. Hence after the interaction between the receptor **1** and F^-, the total change in Gibbs free energy is-0.152 kcal/mol. The negative value indicates the feasibility of the sensing process in thermodynamic aspects. The bond angle and bond length of various bonds of $\mathbf{1}^-$ resonate from 118.3-120 Å and 1.395-1.415 Å. As shown in Table 1, C=C bond length increases and C-N bond length decreases, respectively. This may be due to the single bond and double bond character of these bonds in the receptor in the presence of fluoride anion. While the bond angle decreases between C13, N12, H21, and similarly between N12, C11, H22 atoms. All these changes may be attributed to the enhancement of conjugation across the donor-acceptor unit. The IRC parameters, i.e., total energy, bond energy, and bond angle for $\mathbf{1}^-$ are shown below in Fig. 6.

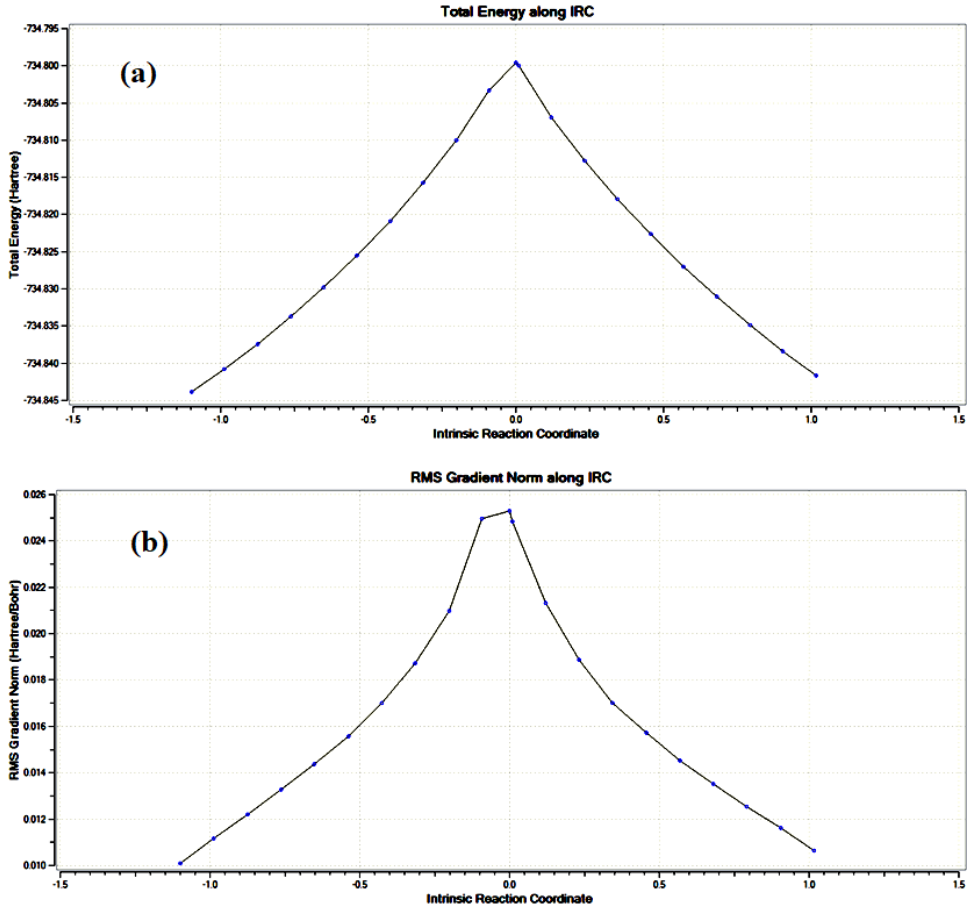

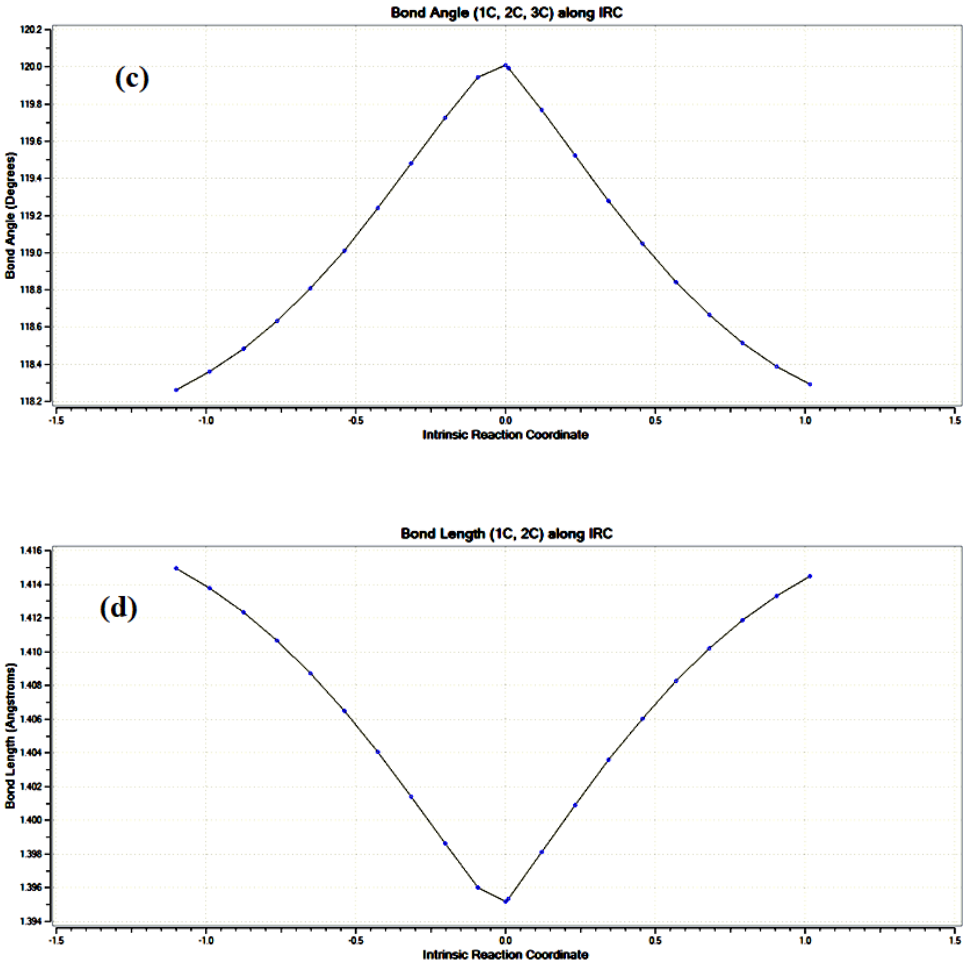

Fig. 6. (a) Theoretically calculated total energy, (b) Gibbs energy, (c) bond angle, and (d) bond length of the deprotonated for the receptor $\mathbf{1}^{-}$.

4. Conclusion

In conclusion, we have investigated the sensing mechanism of an anion receptor **1** with the help of quantum computational (DFT/TD-DFT) methods and mainly discussed the ^{1}H NMR and UV–vis spectra. A receptor molecule possessing D-π-A backbone was established to perform prompt colorimetric sensing of F^{-}through PTS signaling mechanism. The sensing of fluoride anion is attributed to their higher basicity or/and hydrogen bonding tendency under polar aprotic environment (THF). The FMOs analysis indicates intermolecular charge transfer (ICT) enhancement through deprotonation. Fluoride-induced deprotonation decreases the HOMO-LUMO energy gap, which correlates to the bathochromic shift in UV-Vis spectra. The PTS mechanism was further

probed through calculated ^{1}H NMR. The experimentally calculated results were in good agreement with the theoretical observations.

Acknowledgments

We thank the Department of Chemistry (GDC Shopian) for providing infrastructure and their support throughout this work and promoting a healthy working environment for research. M. A. Kaloo gratefully acknowledges the Department of Science and Technology, New Delhi, for the INSPIRE-FACULTY award [DST/INSPIRE/04/2016/000098].

References

1. M. Fokkens, T. Schrader, and F. G. Klarner, J. Am. Chem. Soc. **127**, 41 (2005). https://doi.org/10.1021/ja052806a
2. J. W. Jones and H. W. Gibson, J. Am. Chem. Soc. **125**, 12 (2003). https://doi.org/10.1021/ja0689334
3. J. W. Jones, L. N. Zakharov, A. L. Rheingold, and H. W. Gibson, J. Am. Chem. Soc. **124**, 10 (2002). https://dx.doi.org/10.1021/ar500046r
4. P. A. Gale, Chem. Soc. Rev. **39**, 3 (2010). https://doi.org/10.1039/c001871f
5. J. Liu, Y. Liu, Q. Liu, C. Li, L. Sun, and F. Li, J. Am. Chem. Soc. **133**, 12 (2011). https://doi.org/10.1021/ja109659k
6. T. T. Christison and J. S. Rohrer, J. Chromatogr. A, **1155**, 1 (2007). https://doi.org/10.1016/j.chroma.2007.02.083
7. P. D. Beer and P. A. Gale, Angew. Chem. Int. Ed. **40** (2001). https://doi.org/10.1002/1521-3773(20010202)40:3<486::AID-ANIE486>3.0.CO;2-P
8. C. Perez-Casas and A. K. Yatsimirsky, J. Org. Chem.**73**, 2 (2008). https://doi.org/10.1007/s10847-010-9813-5
9. F. Y. Wu, Z. C. Wen, N. Zhou, Y. F. Zhao, and Y. B. Jiang, Org. Lett. **4**, 5 (2002). https://doi.org/10.1039/B926320A
10. J. M. Linares, D. Powell, and J. K. Bowman, Coord. Chem. Rev. **240**, 13 (2003). https://doi.org/10.5155/eurjchem.2.3.410-415.189
11. J. M. Kang, H. S. Kim, and D. O. Jang, Tetrahedron Lett. **46**, 7 (2005). https://doi.org/10.1002/cjoc.200790115
12. K. Chellappan, N. J. Singh, I. C. Hwang, J. W. Lee, and K. S. Kim, Angew Chem. Int. Ed. **44,** 10 (2005). https://doi.org/10.1063/1.2147283
13. N. Ahmed, V. Suresh, B. Shirinfar, I. Geronimo, A. Bist, I. C. Hwang, and K. S. Kim, Org. Biomol. Chem. **10**, 3 (2012). https://doi.org/10.1007/s12274-020-2718-8
14. V. Amendola, L. Fabbrizzi, and L. Mosca, Chem. Soc. Rev. **39,** 9 (2010). https://doi.org/10.1039/B822552B
15. J. R. Farley, J. E. Wergedal, and D. J. Baylink, Sci. **222,** 3 (1983). https://doi.org/10.1007/BF02555092
16. J. M. You, H. Jeong, H. Seo, and S. Jeon, Sens. Actuators B Chem. **146**, 160 (2010).
17. A. Aggeli, M. Bell, L. M. Carrick, C. W. G Fishwick, R. Harding, P. J. Mawer, S. E. Radford, A. E. Strong, and N. Boden, J. Am. Chem. Soc. **125**, 3 (2003). https://doi.org/10.1021/ja021047i
18. I. H. A. Badr and M. E. Meyerhoff, J. Am. Chem. Soc. **127**, 15 (2005). https://doi.org/10.1021/ja0500153
19. M. Melaimi and F. O. P. Gabbai, J. Am. Chem. Soc. **127**, 27 (2005). https://doi.org/10.1021/ja053058s
20. M. A. Kaloo and J. Sankar, Analyst **138**, 3 (2013). https://doi.org/10.1039/C3AN00942D

21. D. Jacquemin and C. Adamo, Computational Molecular Electronic Spectroscopy with TD-DFT (Springer, Berlin, 2015). https://doi.org/10.1007/128_2015_638
22. A. D. Laurent, C. Adamo, and D. Jacquemin, Phys. Chem. Chem. Phys. **16**, 3 (2014). https://doi.org/10.1039/C3CP55336A
23. J. Hossen and T. K. Pal, J. Sci. Res. **13**, 2 (2021). https://doi.org/10.3329/jsr.v13i2.51731
24. G. Gayatri, J. Sci. Res. **13**, 1 (2021). https://dx.doi.org/10.3329/jsr.v13il.48371
25. B. Moorell, A. Charaf-Eddin, A. Planchat, C. Adamo, J. Autschbach, and D. Jacquemin, J. Chem. Theory Comput. **8**, 7 (2014). https://doi.org/10.1021/ct300326f
26. D.Yang, P. Li, R. Zheng, Y. Wang, and J. Lv, Theor. Chem. Acc. **135** (2016). https://doi.org/10.1007/s00214-015-1802-8
27. M. J. Frisch, et al., Gaussian 09. Revision A 02 Gaussian Inc. Wallingford CT (2009).
28. I. S. K. Kerkines and I. D. Petsalakis, J. Phys. Chem. A **115**, 6 (2011). https://doi.org/10.1021/jp1088433
29. M. Takeuchi, T. Shoya, and T. M. Swager, Angew Chem. Int. Ed. **40**, 3372 (2001). https://doi.org/10.1002/1521-3773(20010917)40:18<3372::AID-ANIE3372>3.0.CO;2-1
30. Y. Qu , J. Hua, and H. Tian, Org. Lett. **12**, 4 (2010). https://doi.org/10.1021/ol9029066